



V, I, R measurements: how to generate and measure quantities and then how to get data (resistivity, magnetoresistance, Hall).

**590B**

**Makariy A. Tanatar**

September 25, 2009

## **Resistivity**

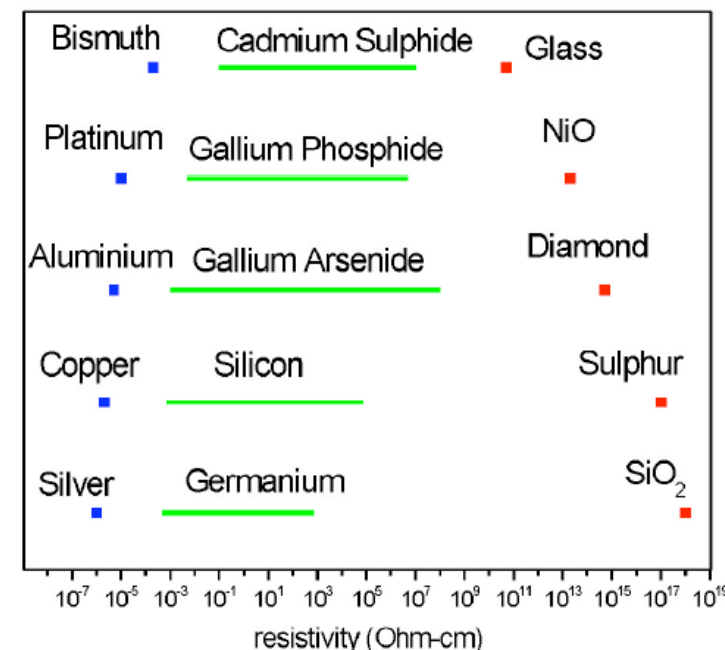
**Typical resistivity temperature dependence:  
metals, semiconductors**

**Magnetic scattering**



# Resistivities of Real Materials

Material	Resistivity 20°C
Silver	1.59 $\mu\Omega$ cm
Copper	1.72 $\mu\Omega$ cm
Aluminum	2.82 $\mu\Omega$ cm
Tungsten	5.8 $\mu\Omega$ cm
Platinum	11 $\mu\Omega$ cm
Manganin	48 $\mu\Omega$ cm
Constantan	49 $\mu\Omega$ cm
Nichrome	110 $\mu\Omega$ cm
Germanium	4.6
Glass	$10^8$ - $10^{12}$ $\Omega$ cm
PET	$10^{18}$ $\Omega$ cm
Teflon	$10^{20}$ - $10^{22}$ $\Omega$ cm



**Most semiconductors in their pure form are not good conductors, they need to be doped to become conducting.**

**Not all so called “ionic” materials like oxides are insulators.**



➤ We can relate the conductivity,  $\sigma$ , of a material to microscopic parameters that describe the motion of the electrons (or other charge carrying particles such as holes or ions).

➤  $\sigma = ne(e\tau/m^*)$

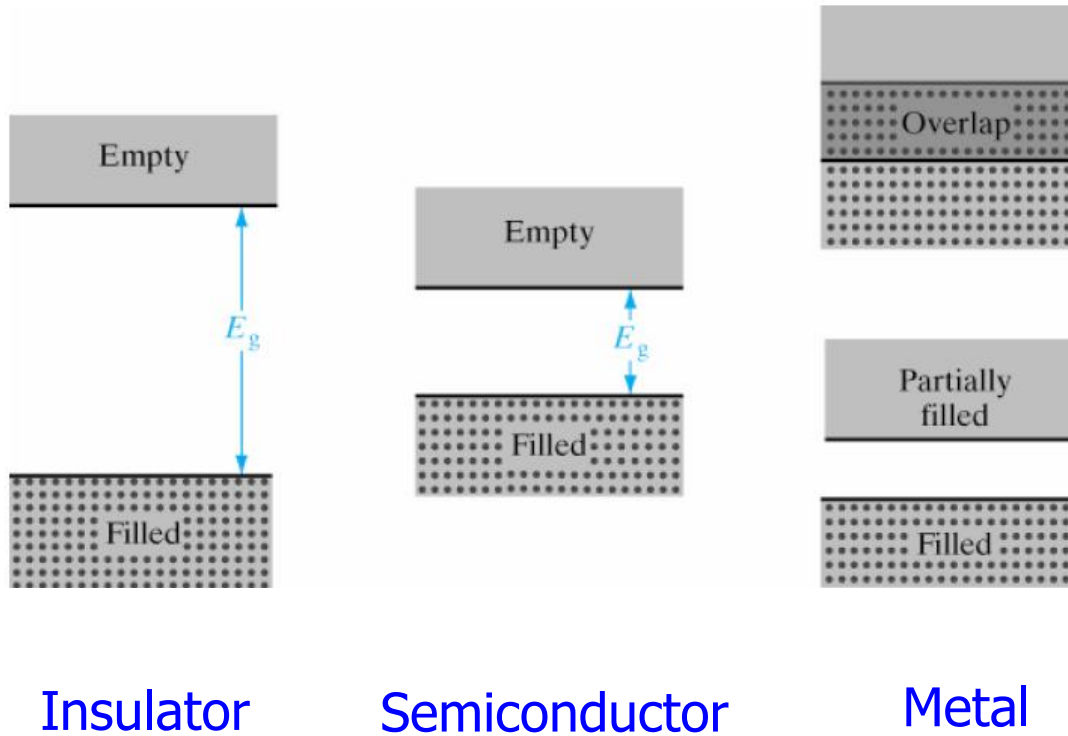
➤  $\mu = e \tau /m^*$

➤  $\sigma = ne \mu$

- where
- $n$  = the carrier concentration ( $\text{cm}^{-3}$ )
  - $e$  = the charge of an electron =  $1.602 \times 10^{-19} \text{ C}$
  - $\tau$  = the relaxation time (s) {the time between collisions}
  - $m^*$  = the effective mass of the electron (kg)
  - $\mu$  = the electron mobility ( $\text{cm}^2/\text{V}\cdot\text{s}$ )

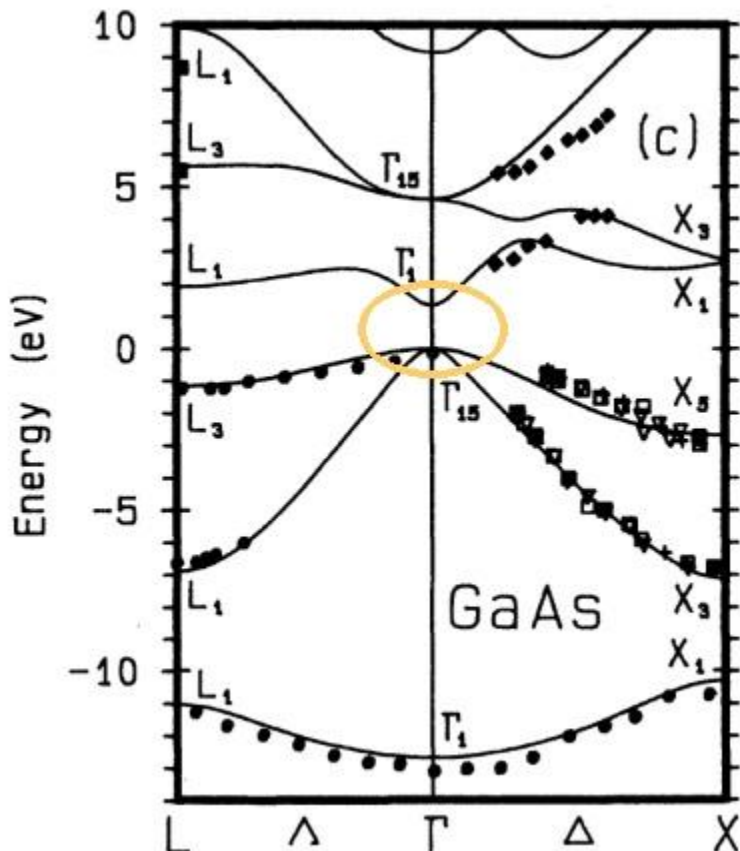


# Metals, Semiconductors & Insulators

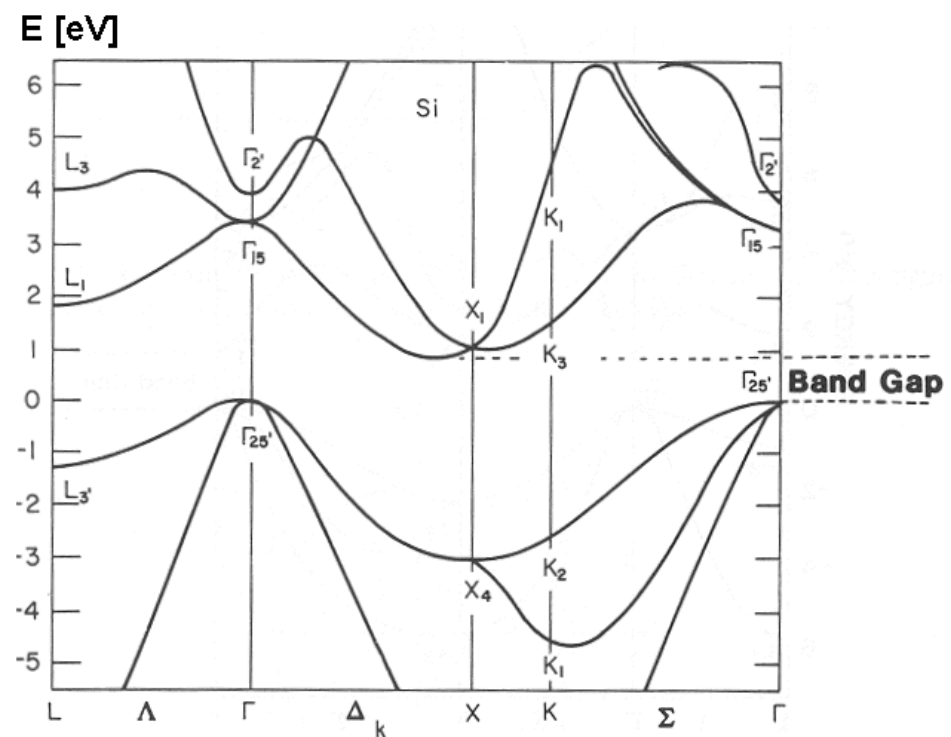


Big variation is due to big difference in free carrier density

# Energy bands in semiconductors



Direct-gap  
III-V  
II-VI



Indirect band-gap  
Si, Ge

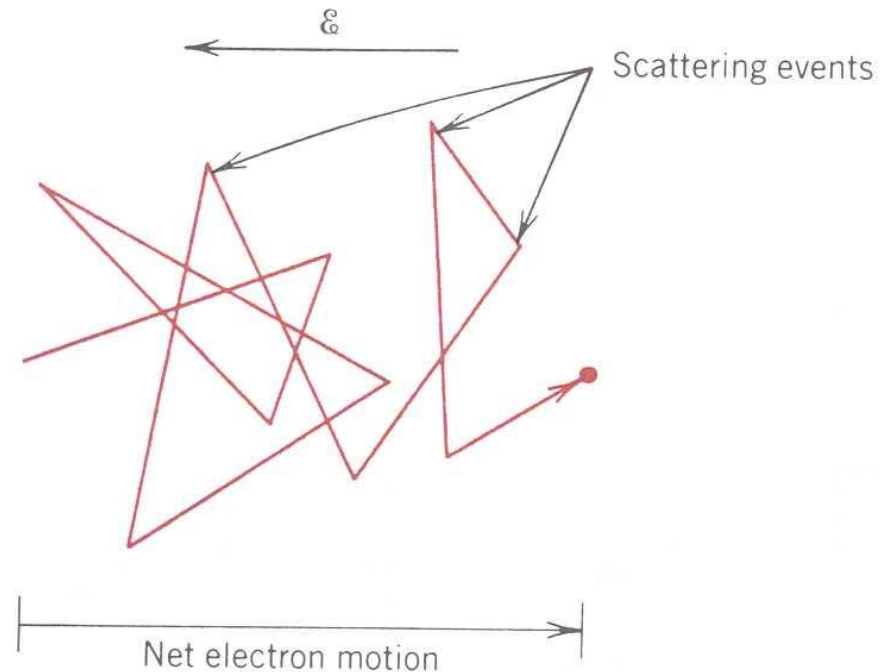
Compound	Structure	Bandgap (eV)	$e^-$ mobility (cm <sup>2</sup> /V-s)	$h^+$ mobility (cm <sup>2</sup> /V-s)
Si	Diamond	1.11 (I)	1,350	480
Ge	Diamond	0.67 (I)	3,900	1,900
AlP	Sphalerite	2.43 (I)	80	---
GaAs	Sphalerite	1.43 (D)	8,500	400
InSb	Sphalerite	0.18 (D)	100,000	1,700
AlAs	Sphalerite	2.16 (I)	1,000	180
GaN	Wurtzite	3.4 (D)	300	---

# Electron mobility and scattering

What scatters carriers?

Disruptions in periodicity

- defects
- lattice vibrations
- surfaces



- **Thermal energy** ⇒ some electrons are excited from the valence band into the conduction band ⇒ **conduction electrons**

- This leaves an empty state in the valence band — a **hole**
  - $n$ : density of CE
  - $p$ : density of holes

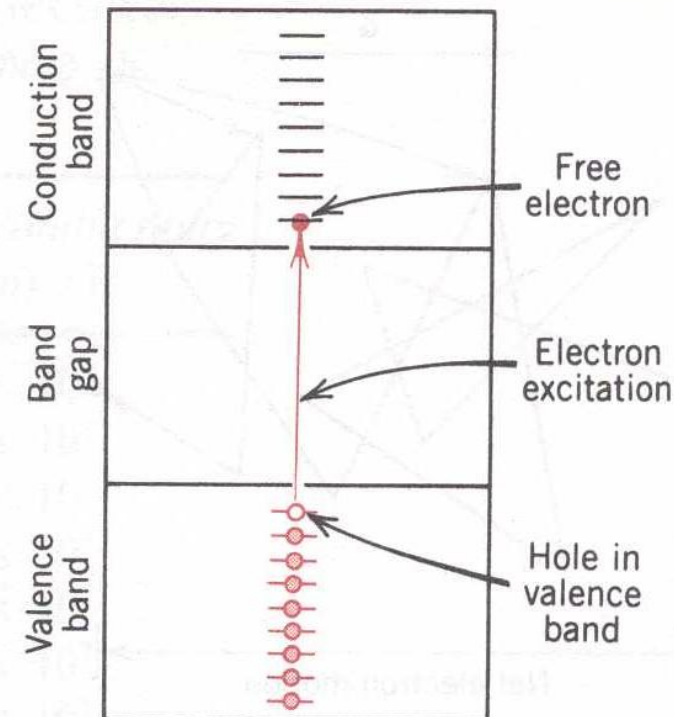
$$n \cdot p = N_C N_V \exp\left(-\frac{E_g}{k_B T}\right)$$

- Intrinsic semiconductor: electrons and holes form in pairs

$$n_i = p_i = \sqrt{N_C N_V} \exp\left(-\frac{E_g}{2k_B T}\right)$$

- Conductivity:

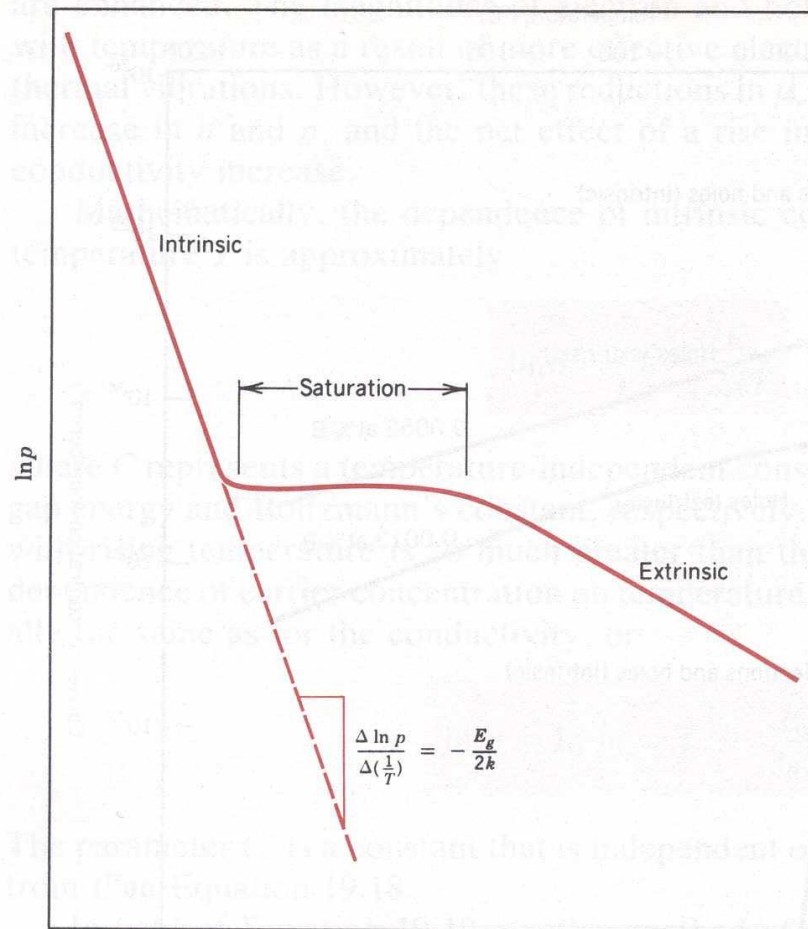
$$\sigma = n_i e \mu_e + p_i e \mu_h = n_i e (\mu_e + \mu_h)$$





## Carrier density

- Low T: **ionization** of dopants
  - *n*-type: donor atoms donate  $e^-$  to conduction band
  - *p*-type: acceptor atoms accept  $e^-$  from valence band
- Intermediate T: all dopants ionized
  - *n*-type: **exhaustion** of donors
  - *p*-type: **saturation** of acceptors
- High T: intrinsic behavior



Schematic plot of the natural logarithm of hole concentration as a function of the reciprocal of absolute temperature for a *p*-type semiconductor that exhibits extrinsic, saturation, and intrinsic behavior.



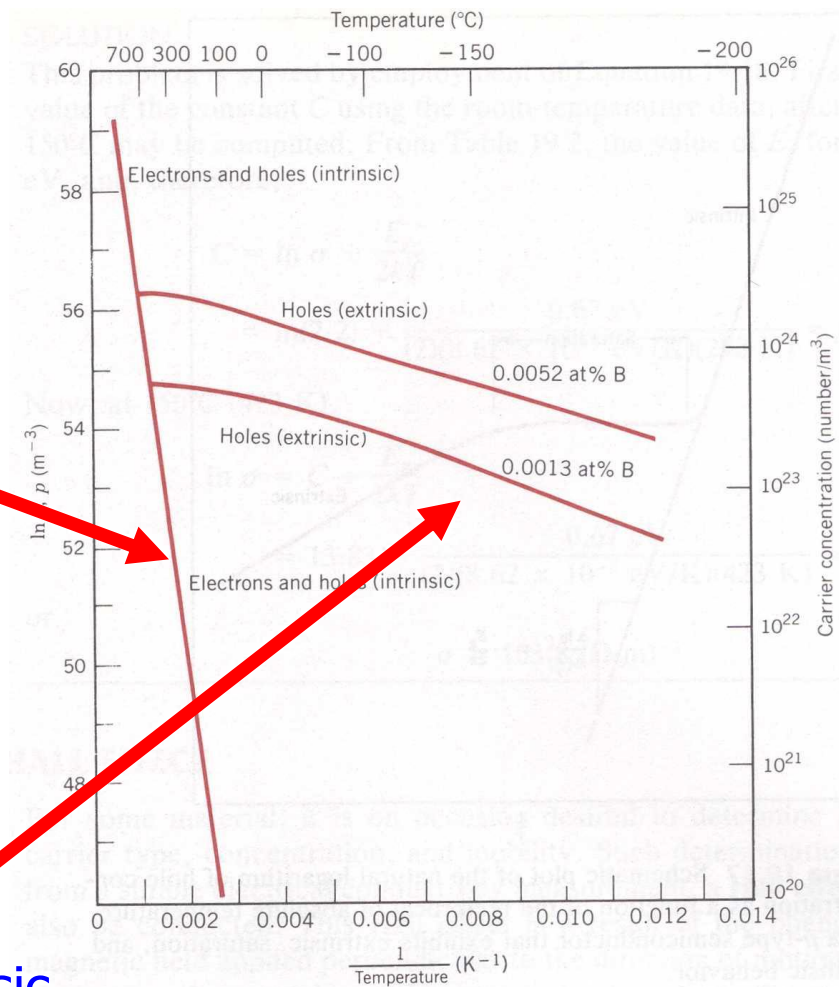
Can obtain bandgap for intrinsic region

$$n = p = \sqrt{N_C N_V} \exp\left(-\frac{E_g}{2k_B T}\right)$$

Intrinsic

Extrinsic

If density of dopants  $N >> n, p$   
Behaves like extrinsic conductor



The logarithm of carrier (electron and hole) concentration as a function of the reciprocal of the absolute temperature for intrinsic silicon and two boron-doped silicon materials.  
(Adapted from G. L. Pearson and J. Bardeen, *Phys. Rev.*, **75**, 865, 1949.)

$$\sigma = n e \mu_e + p e \mu_h \approx n e \mu_e = N_d e \mu_e$$

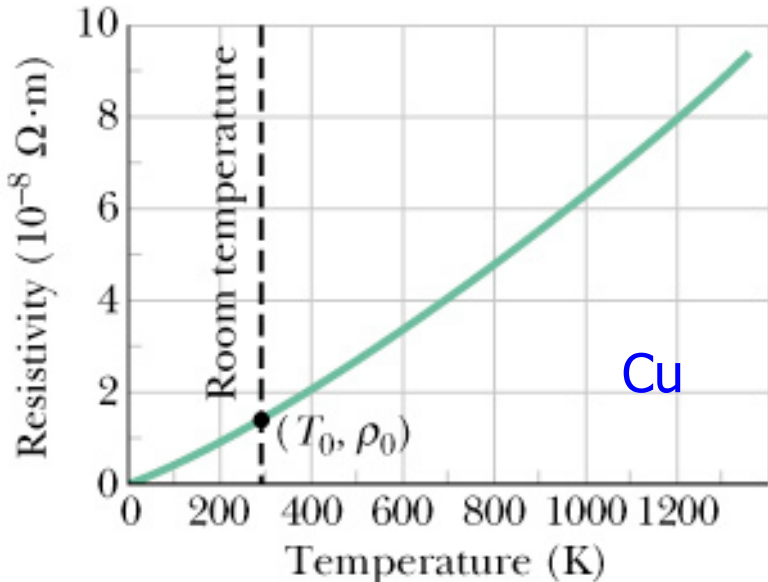


# Metals

D. MATTHIESSEN's RULE

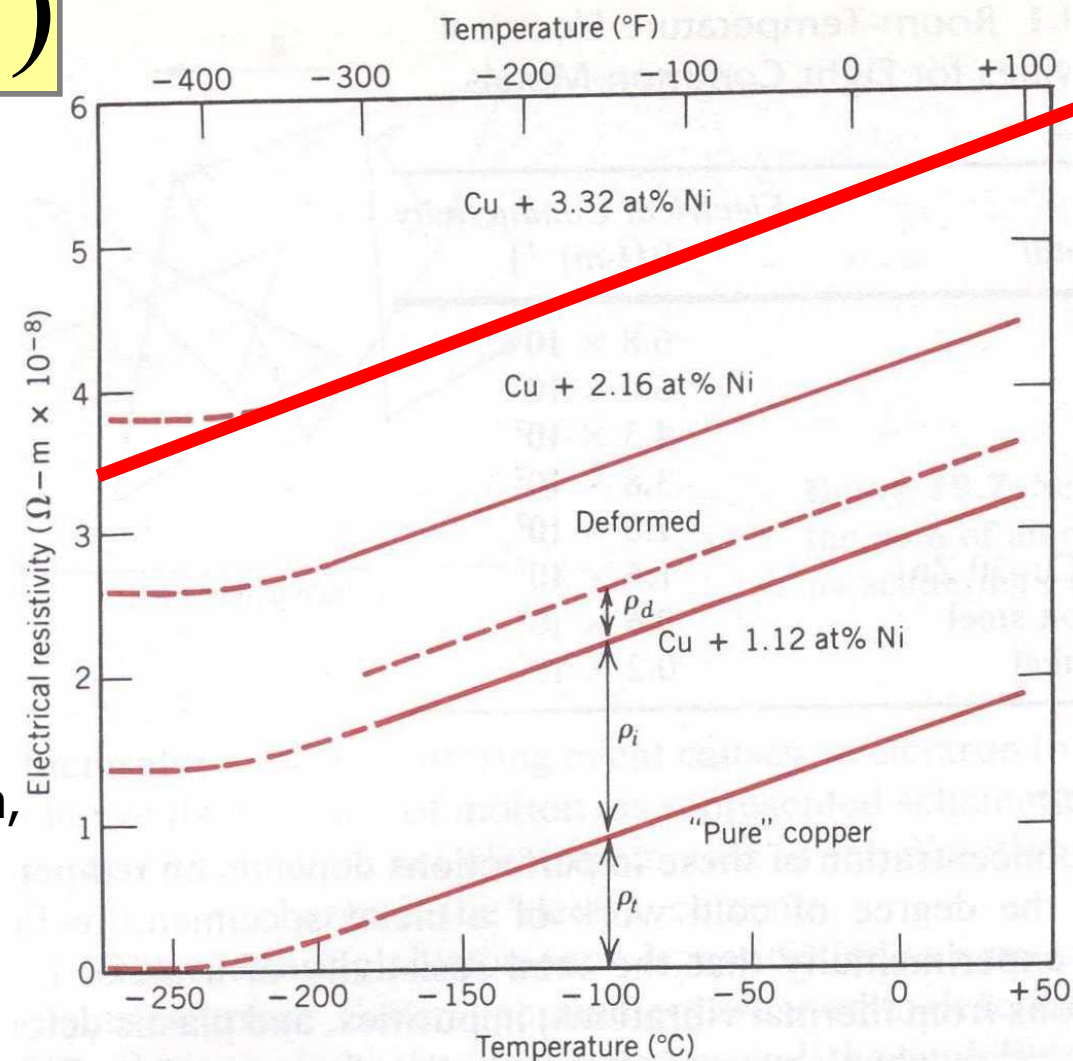
$$R = R_0 + R_T,$$

$$\rho - \rho_0 = \rho_0 \alpha (T - T_0)$$



Temperature coefficient of resistivity  $\alpha$  reflects electron-phonon interaction, property of material

- Thermal vibrations scatter carriers
- $\Rightarrow$  mobility  $\downarrow$
- $\Rightarrow$  conductivity  $\downarrow$
- $\Rightarrow$  resistivity  $\uparrow$





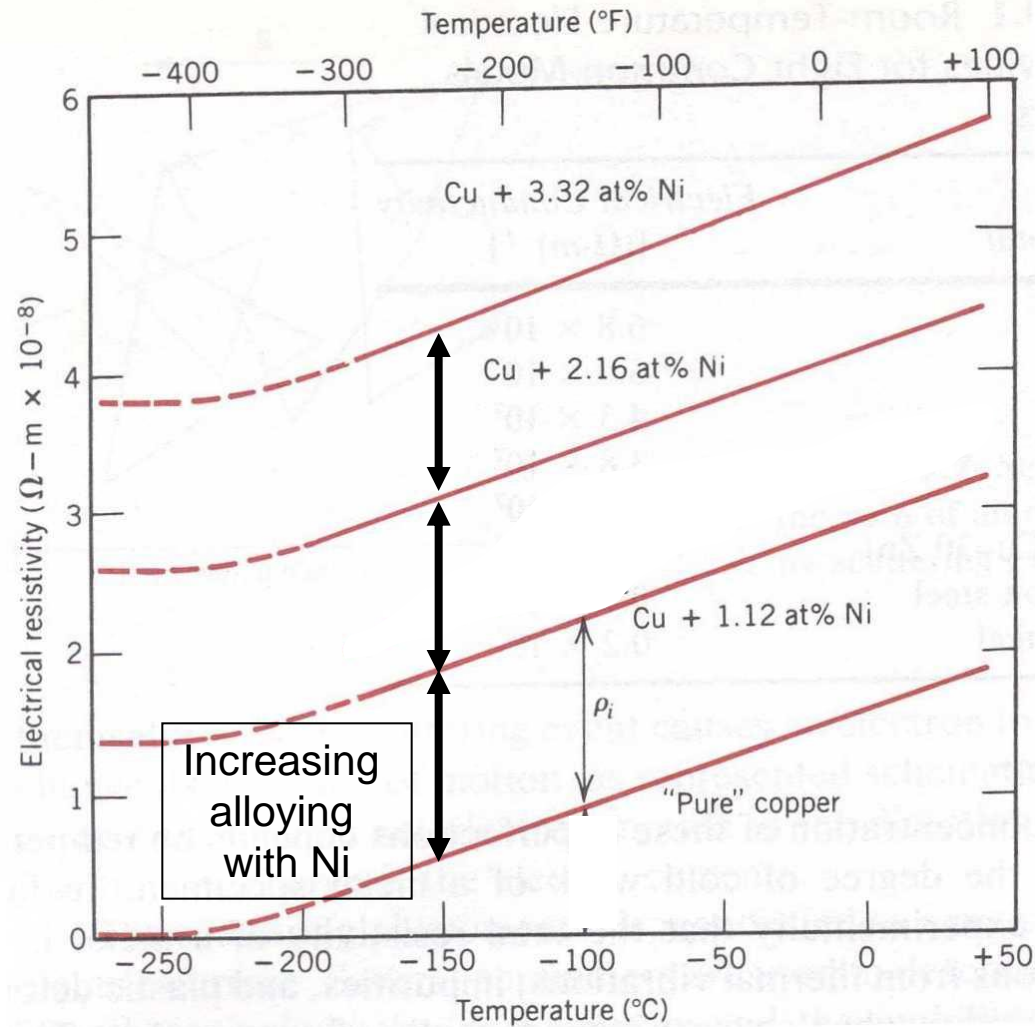
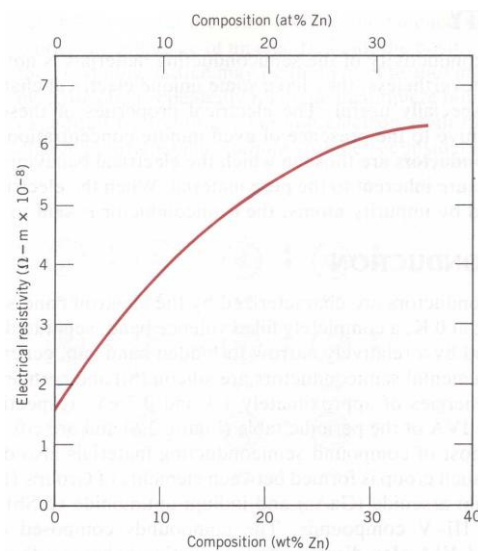
## D. MATTHIESSEN's RULE

$$R = R_0 + R_T,$$

- Effect of **impurities** on  $\mu$

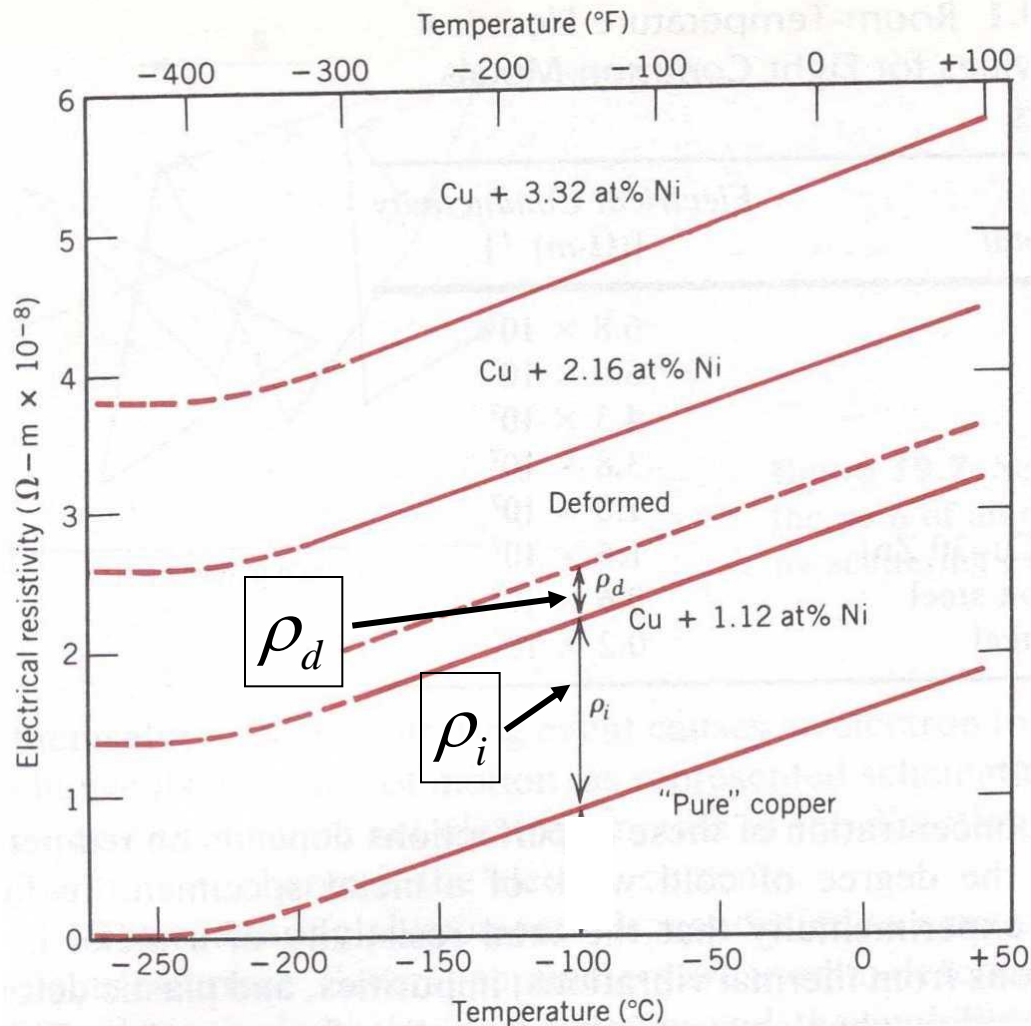
$$\rho_i = A c_i (1 - c_i)$$

- $A$ : property of host and impurity
- $c_i$ : atomic fraction of impurity



➤ Effect of ***deformation*** on  $\mu$

- Dislocations (regions of deformed material) scatter carriers, increasing the electrical resistivity by  $\rho_D$





## Resistivity temperature dependence of metals closer look

High temperature

$$\rho - \rho_0 = \rho_0 \alpha (T - T_0)$$

$T >> \Theta_D$  density of phonons  $\sim T$

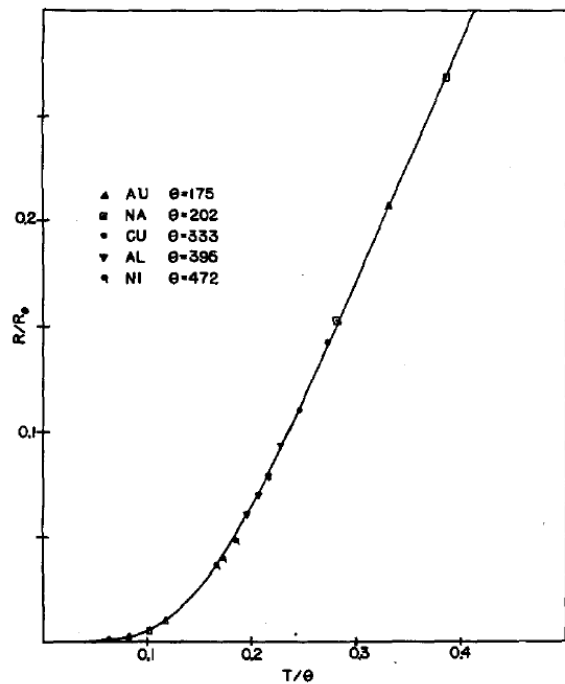
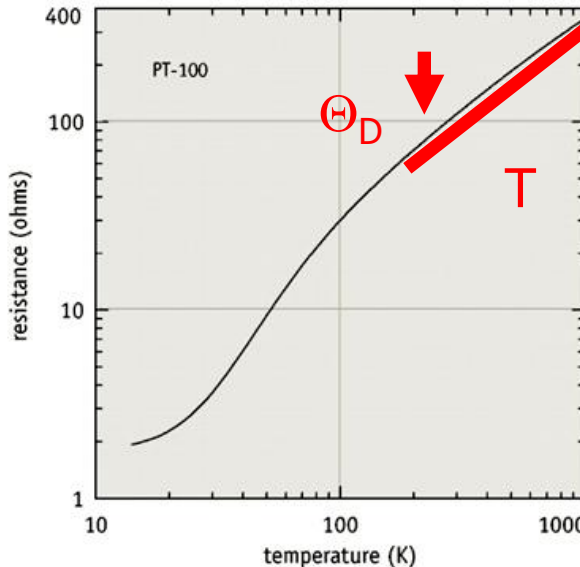
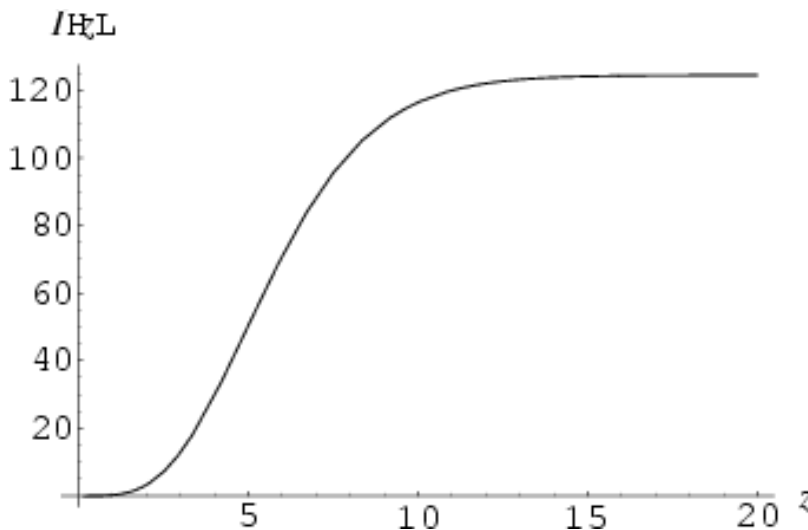


FIG. 1. Temperature variation of resistance of various metals. The curve is a plot of the Bloch-Gruneisen function (Eq. (28)). Data from values quoted by Meissner (cf. Bibliography).



$T < \Theta_D$  spectrum of phonons changes  
 Bloch-Gruneisen law  
 For most of metals  
 $R = R_0 f(T/\Theta)$ ,  
 $\Theta$  is close to Debye temperature  
 in specific heat, not the same due to  
 selectivity of scattering

$$\rho(T) = \rho(0) + A \left( \frac{T}{\Theta_R} \right)^n \int_0^{\frac{\Theta_R}{T}} \frac{x^n}{(e^x - 1)(1 - e^{-x})} dx$$



$\propto T$

$$\rho_{ph} \sim f(q) S_{ph}$$

With some  
“filtering” due to  
 $q$ -dependence of  
scattering probability

### Comparison of $\Theta_R$ and $\Theta_D$

Metal	Ag	Au	Al	Cu	Pd	Pt	Rh
$\Theta_R$	200	200	395	320	270	240	340
$\Theta_D$	220	185	385	320	300	225	350

After G. T. Meaden Electrical Resistance of Metals

$q=0$  at  $T=0$

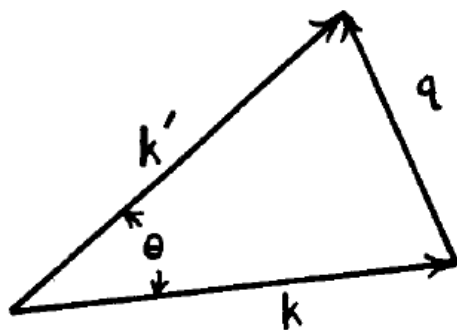


FIG. 11. Illustrating the vector relations for the scattering of an electron wave by a lattice wave.

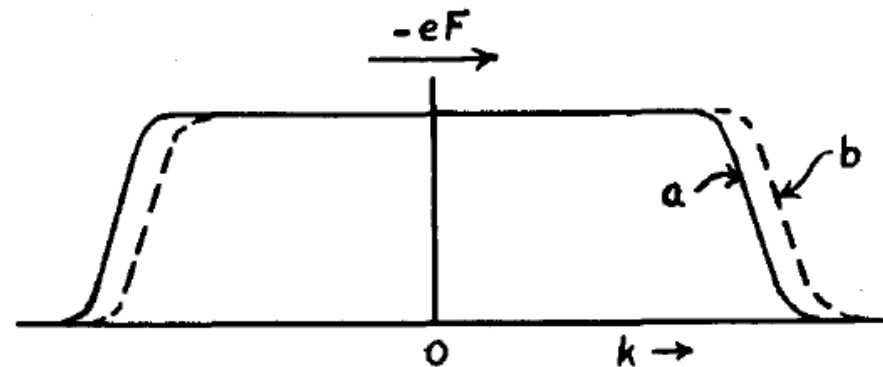


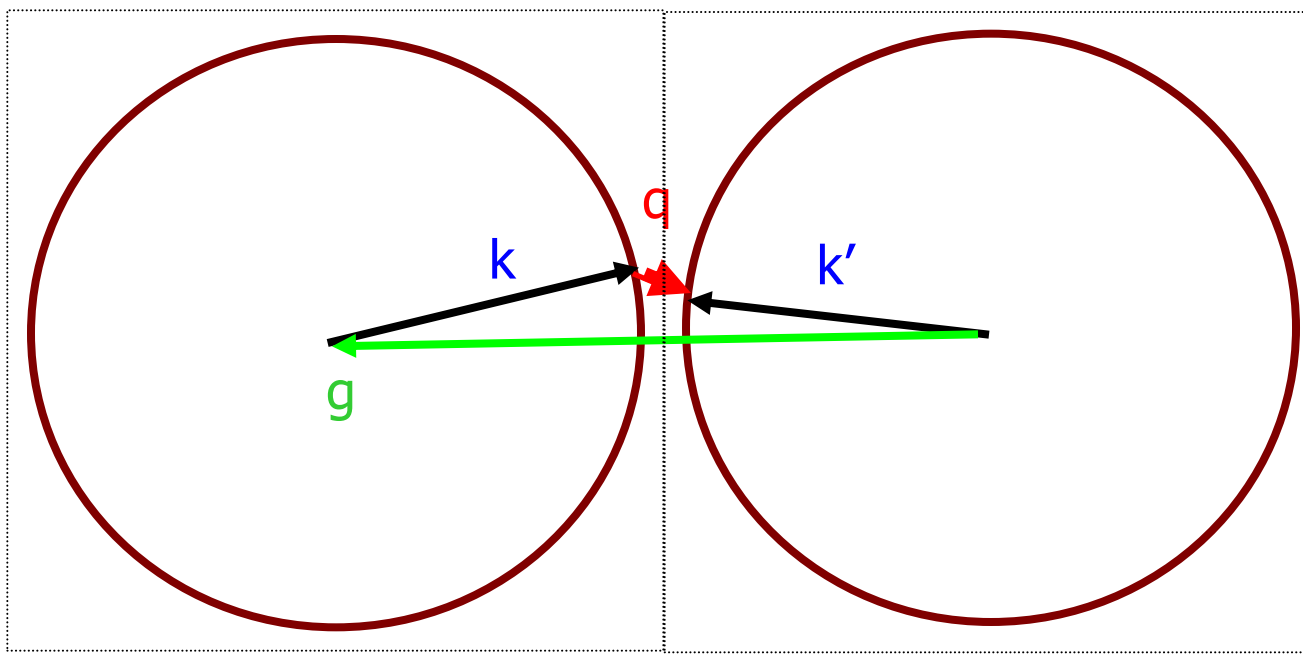
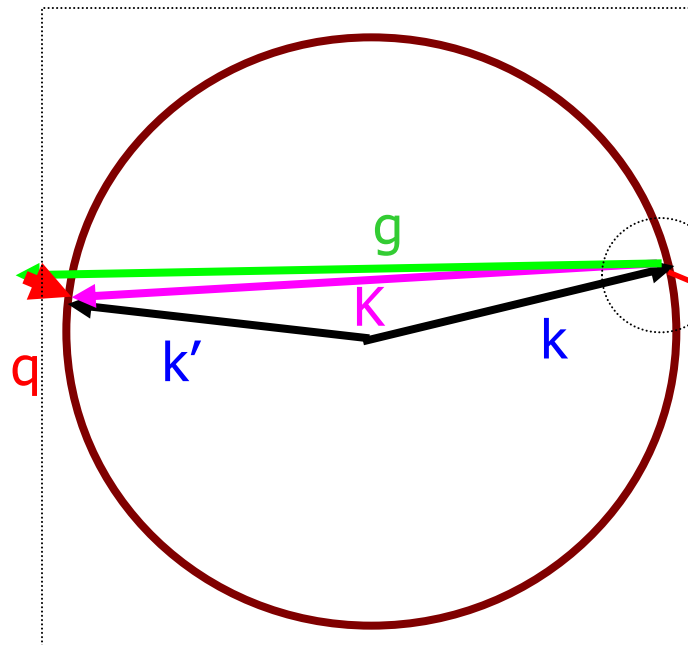
FIG. 9. Shift of the electron distribution due to an applied field.

Direct electron scattering on phonons at low temperatures does not contribute much to resistivity, electrons can not scatter at large angle due to momentum conservation law

The only efficient way: Umklapp processes, scattering with momentum transfer to reciprocal lattice



## Umklapp processes





# Electron-electron scattering

At low temperatures

$$\rho = \rho_0 + \alpha T^n$$

$$n=5 \text{ e-ph}$$

Not very efficient in scattering

In e-e scattering total momentum is conserved

Scattering does not contribute to resistivity

- Umklapp

- Electrons from different bands  
s-d scattering

$$\sigma = (Ne^2/m)(\alpha\tau_a + \beta\tau_b).$$

Bands a and b, densities  $\alpha$  and  $\beta$

Relaxation times  $\tau_a$  and  $\tau_b$

Mott:  $\tau_a$  and  $\tau_b$  are of the same order of magnitude;

$\alpha$  and  $\beta$  can be very different,

High probability of scattering into large DOS band

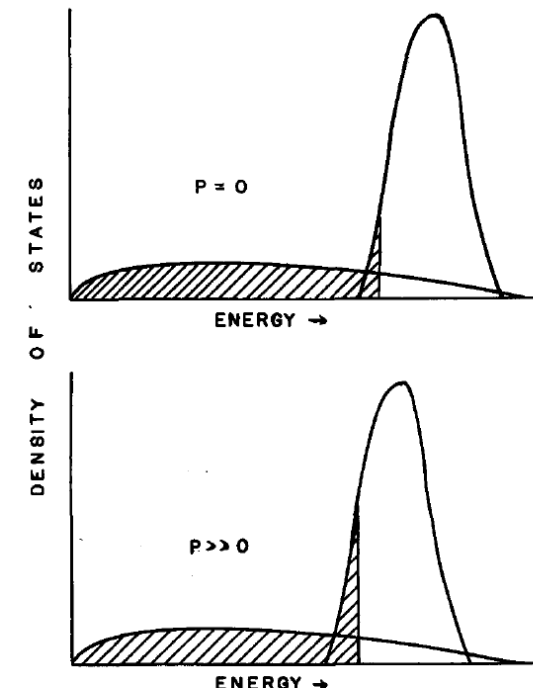


FIG. 14. Occupied electronic states in two overlapping bands at (a) zero pressure, (b) some high pressure (schematic).

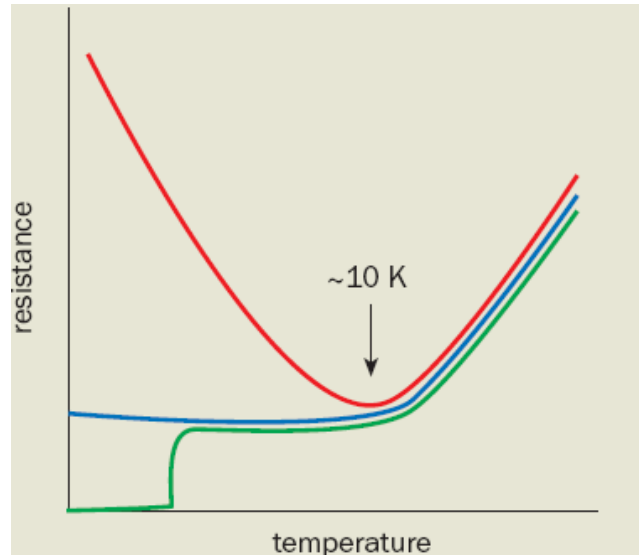
$$n=2 \text{ e-e}$$

$$n=3 \text{ s-d}$$



## Kondo effect

Dilute magnetic impurities in metals



ASAHI SHINBUN

Interaction of conduction electrons with magnetic impurities

Characteristic temperature  $T_K$   
(varies a lot! From 0.1mK Mn in Au  
to 300K V in Au, usually  $\sim 10$  K)

Specific heat per impurity  $C \sim T/T_K$   
Impurity spins completely screened  
at low temperatures

Journal of the Physical Society of Japan  
Vol. 74, No. 1, January, 2005, pp. 1–3  
©2005 The Physical Society of Japan



The theory that describes the scattering of electrons from a localized magnetic impurity was initiated by the work of Jun Kondo in 1964

b. 1930

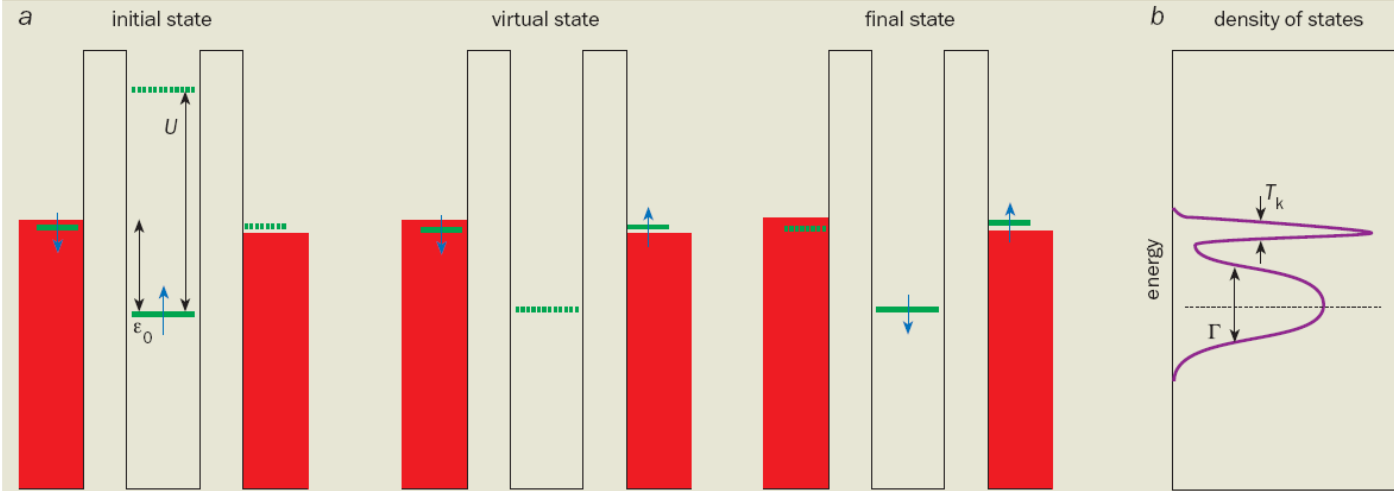
**Revival of the Kondo effect**  
**Leo Kouwenhoven and Leonid Glazman**

PHYSICS WORLD JANUARY 2001

SPECIAL TOPICS

# Anderson impurity model

## 2 Spin flips



(a) The Anderson model of a magnetic impurity assumes that it has just one electron level with energy  $\epsilon_0$  below the Fermi energy of the metal (red). This level is occupied by one spin-up electron (blue). Adding another electron is prohibited by the Coulomb energy,  $U$ , while it would cost at least  $|\epsilon_0|$  to remove the electron. Being a quantum particle, the spin-up electron may tunnel out of the impurity site to briefly occupy a classically forbidden “virtual state” outside the impurity, and then be replaced by an electron from the metal. This can effectively “flip” the spin of the impurity. (b) Many such events combine to produce the Kondo effect, which leads to the appearance of an extra resonance at the Fermi energy. Since transport properties, such as conductance, are determined by electrons with energies close to the Fermi level, the extra resonance can dramatically change the conductance.

Peak in DOS  
Bound to  $E_F$   
additional scattering

$$\rho/\rho_0 = f(T/T_K)$$

universal function of one parameter  $T_K$

$$\rho \sim \ln T$$

**Revival of the Kondo effect**  
**Leo Kouwenhoven and Leonid Glazman**



# Magnetic scattering

$Ce_{1-x}La_xRhIn_5$

f-electrons are localized

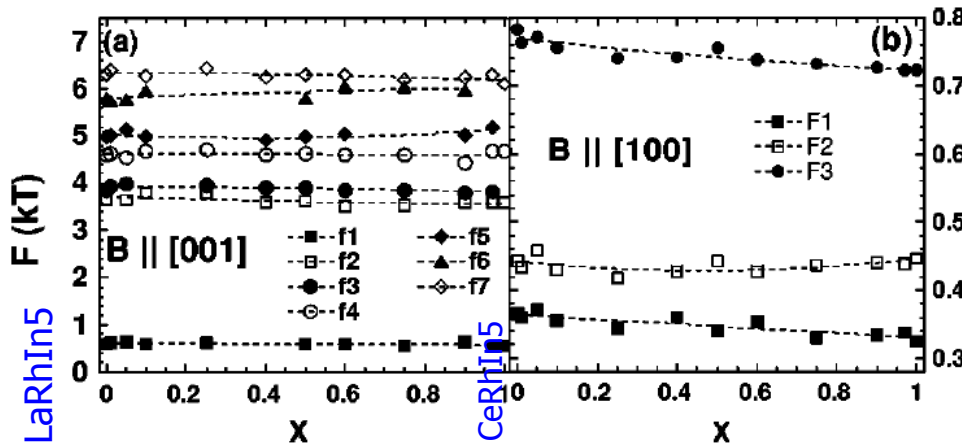


FIG. 2. The principal dHvA frequencies in  $Ce_xLa_{1-x}RhIn_5$  plotted versus  $x$ , (a) for  $B$  applied along [001] and (b) for  $B$  applied along [100].

Same lattice  
localized f-electrons  
add to scattering

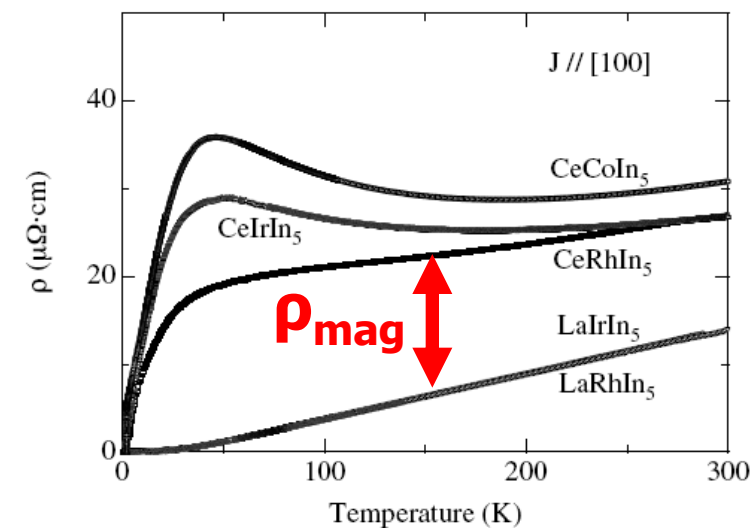
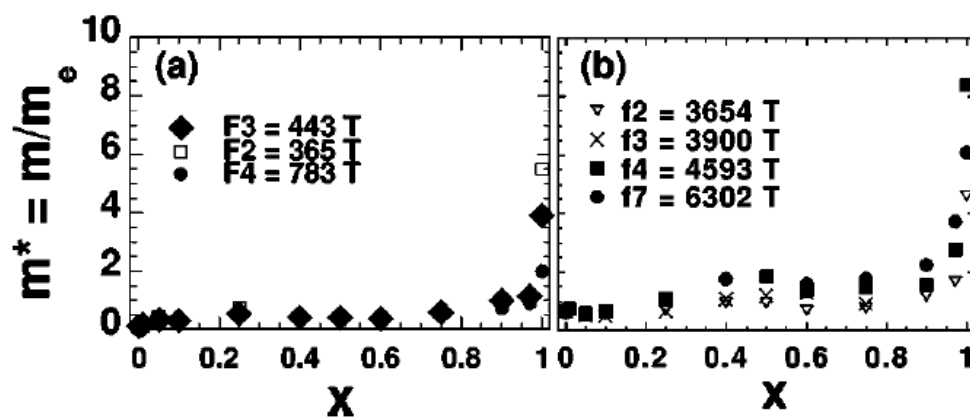


Fig. 3. Temperature dependence of the electrical resistivity in  $RTIn_5$ .



# CeRhIn5

$$\rho_{\text{mag}} \sim S_{\text{mag}}$$

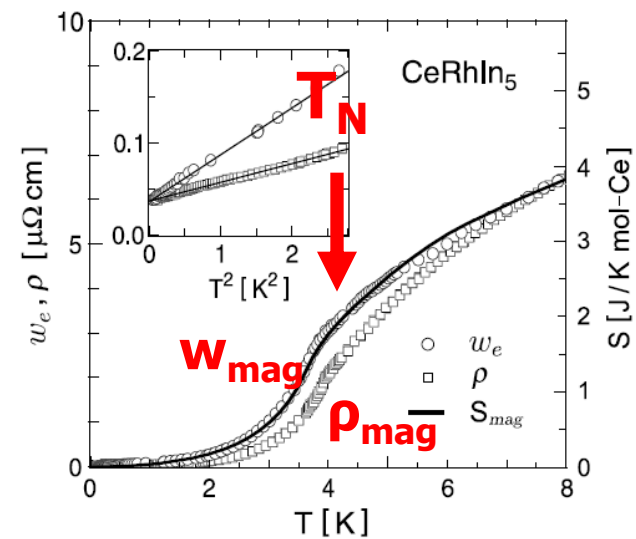
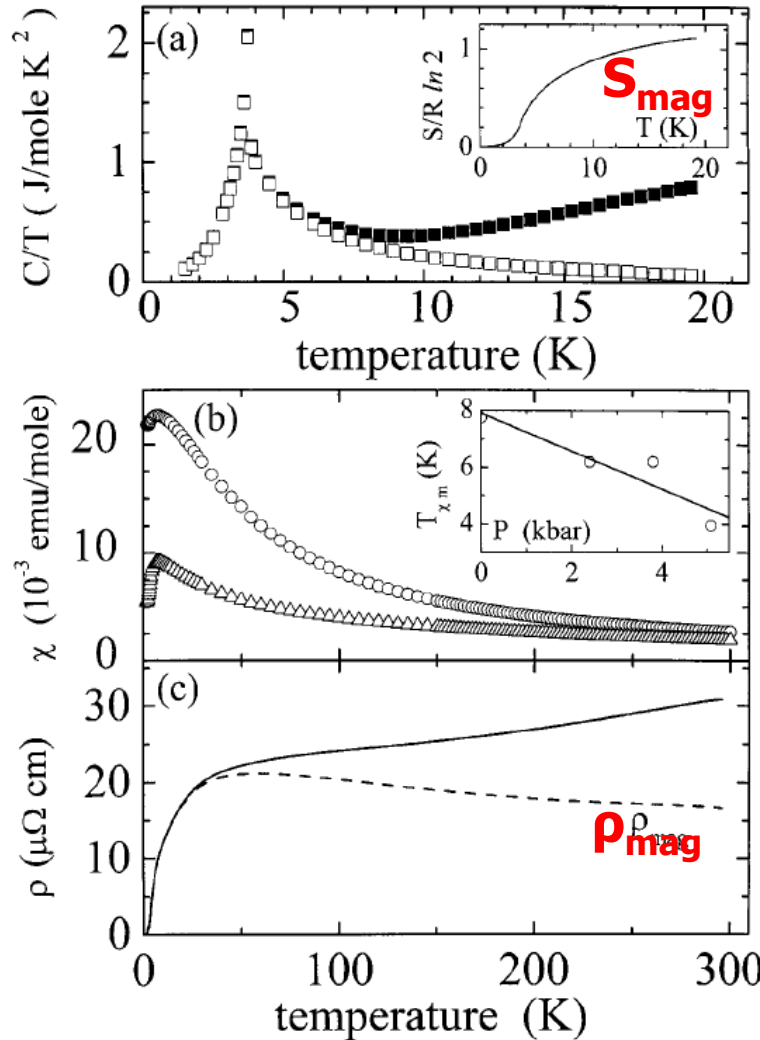
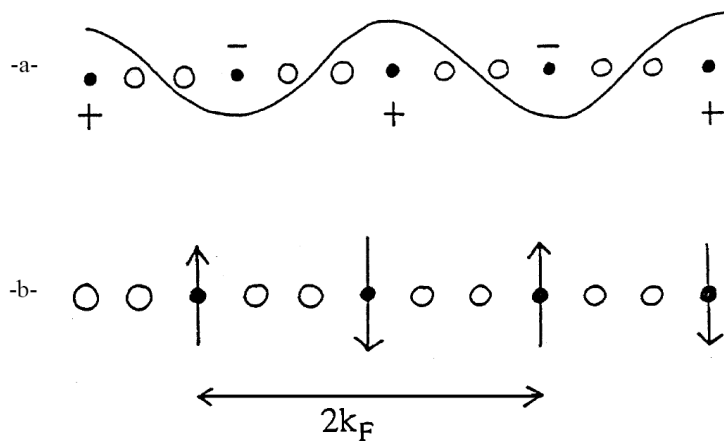
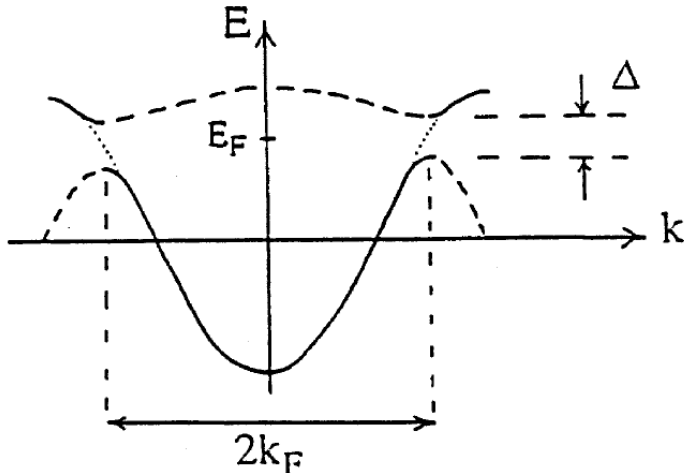


FIG. 2. Electronic thermal resistivity  $w_e$  (circles) and electrical resistivity  $\rho$  (squares), compared to the magnetic entropy  $S_{\text{mag}}$  (line) obtained from published specific heat data [12]. Inset: low-temperature data as a function of  $T^2$ . Lines are linear fits.

“q-filtering” removed:  
Full scattering directly  
proportional to entropy

# Density waves

Rudolph Peierls  
1907-1995



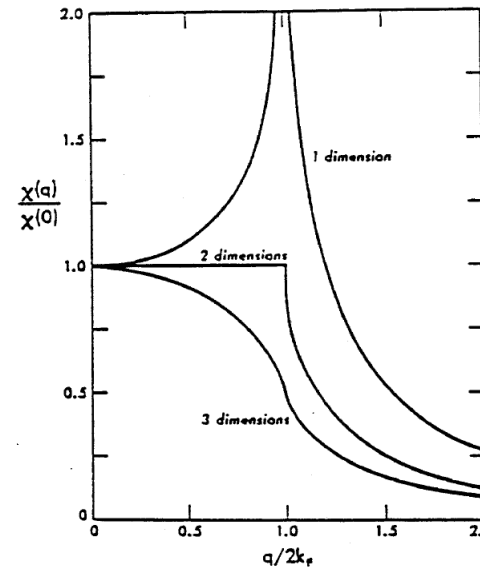
Distortion with  $2K_F$  periodicity  
Decreases electron energy

"Frisch-Peierls Memorandum" of March 1940,  
proposing a "super-bomb which utilizes the  
energy stored in atomic nuclei as a  
source of energy."  
1957 on request of US government removed  
security clearance, suspected of spying

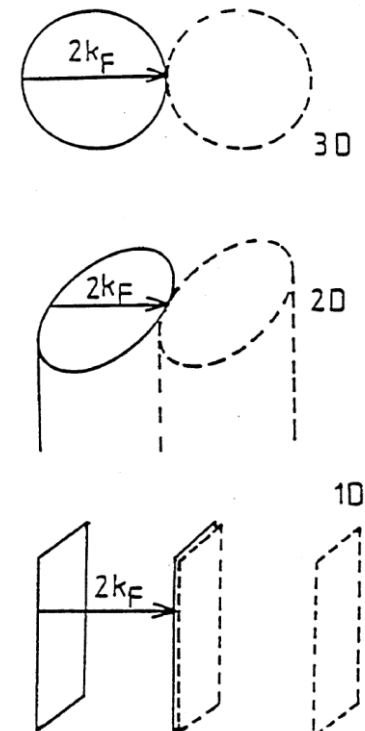
Klaus Fuchs

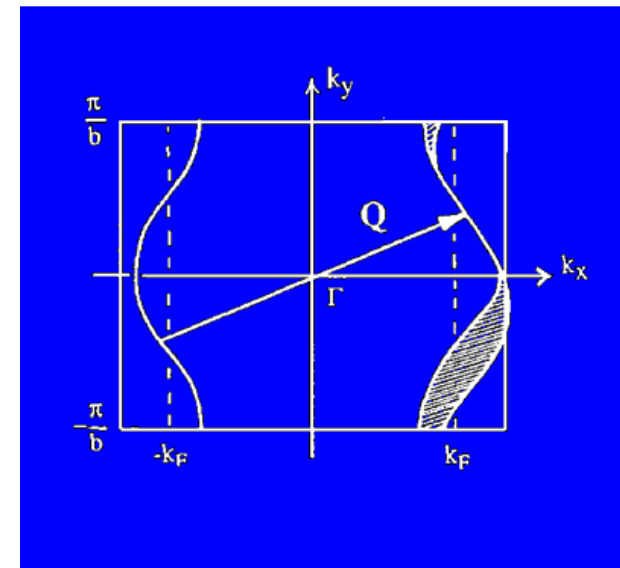
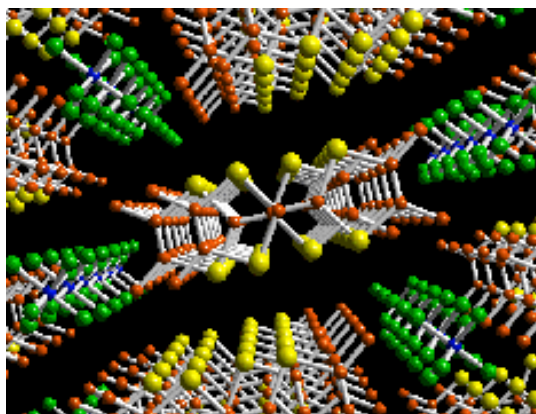
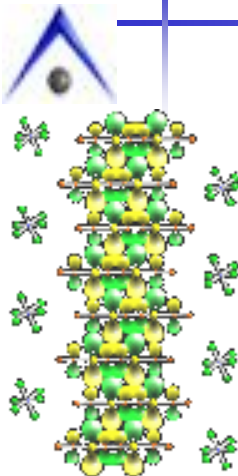
knighted in 1968

[www.history.bham.ac.uk/research/index.htm](http://www.history.bham.ac.uk/research/index.htm)



BCS-like solution  
 $\Delta=1.75 T_c$





The Fermi surface of a quasi-1D conductor  
with distinct parts at  $+k_F$  and  $-k_F$  (here in a cut view).  
**Q** nest one part to another by translation.

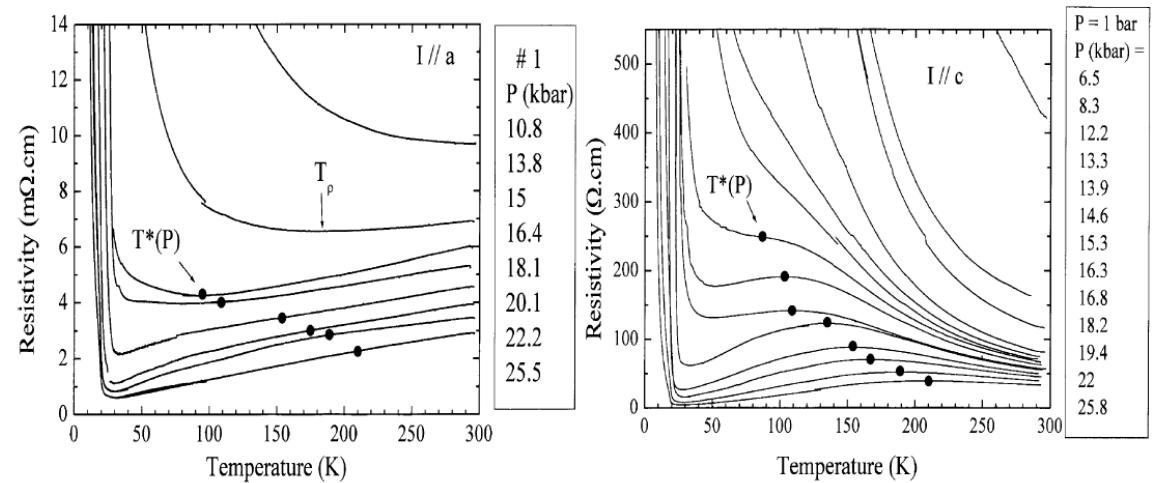
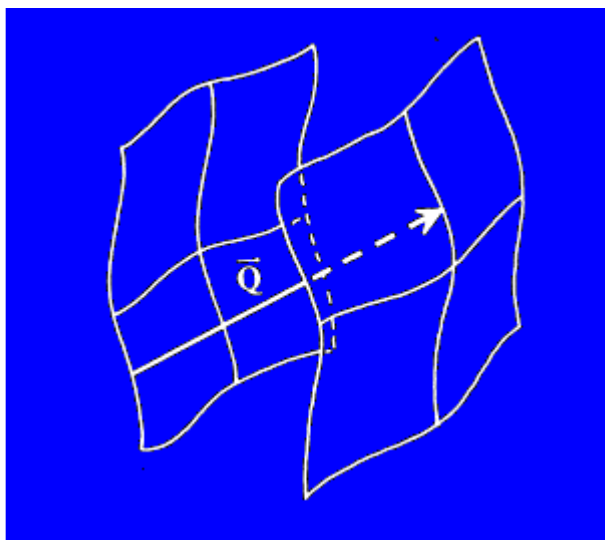


Fig. 2.  $(\text{TMTTF})_2\text{PF}_6$  longitudinal (left) and transverse (right) resistances versus temperature at different pressures.<sup>12</sup>

# Density waves: increasing dimensionality

## Chain

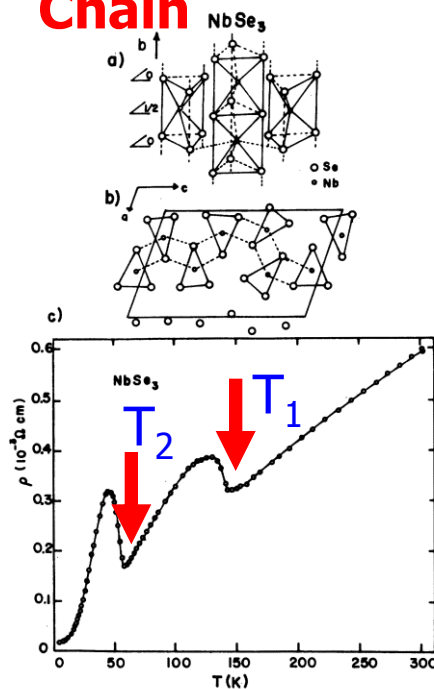


FIG. 1. (a) Crystal structure of  $\text{NbSe}_3$  along the  $b$  axis. The  $\text{Nb}$  atoms in adjacent chains are displaced by half a lattice spacing along  $\vec{b}$  with respect to each other. (b) Crystal structure of  $\text{NbSe}_3$  in the  $a-c$  plane. The unit cell, comprised of six prisms and represented by the parallelogram, has the dimensions  $a = 10.006 \text{ \AA}$ ,  $b = 3.478 \text{ \AA}$ ,  $c = 15.626 \text{ \AA}$ ,  $\beta = 109.30^\circ$ . The  $\text{Nb-Nb}$  distance along  $\vec{b}$  is  $3.478 \text{ \AA}$  (compared to  $2.68 \text{ \AA}$  in the metal). In the other directions it varies from  $4.45$  to  $4.25 \text{ \AA}$ . The dashed lines connect  $\text{Nb}$  and  $\text{Se}$  atoms in the same plane. (c) Resistivity of  $\text{NbSe}_3$  vs temperature. The phase transitions at  $145 \text{ K}$  and  $59 \text{ K}$  have been tentatively identified with the formation of charge-density waves.

## $\text{NbSe}_3$

$$T_1 = 142 \text{ K} \quad \text{ICDW1} \quad q_1 = (0.245 \pm 0.007) \text{ } b^*$$

$$T_2 = 58 \text{ K} \quad \text{ICDW2} \quad q_2 = (0.494 \pm 0.008) \text{ } a^* + (0.267 \pm 0.007) \text{ } b^* + 0.50 \text{ } c^*$$

## Layer

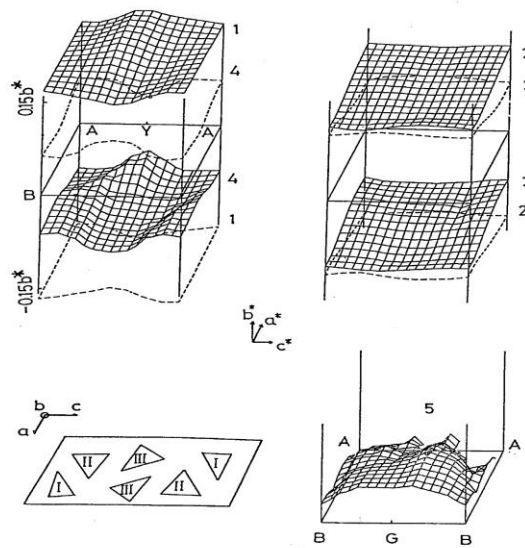


Fig. 1. Fermi surfaces corresponding to each conduction bands and the chain location in a unit cell of  $\text{NbSe}_3$ . The nesting pairs, 1–4 and 2–3, are pictured in half of the Brillouin zone. Each of the nesting pieces of the Fermi surfaces is drawn in the solid and dashed line. Fermi surface 5 is pictured in quarter of the Brillouin zone.

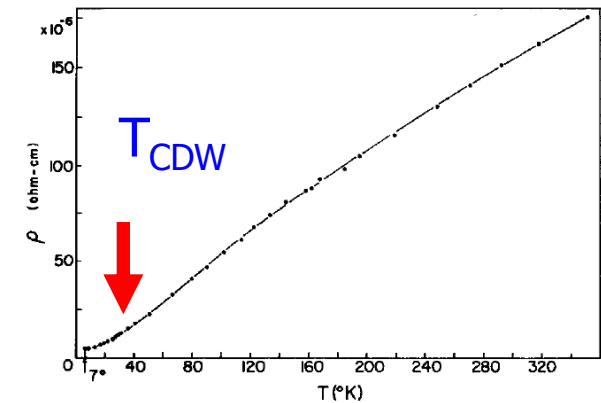
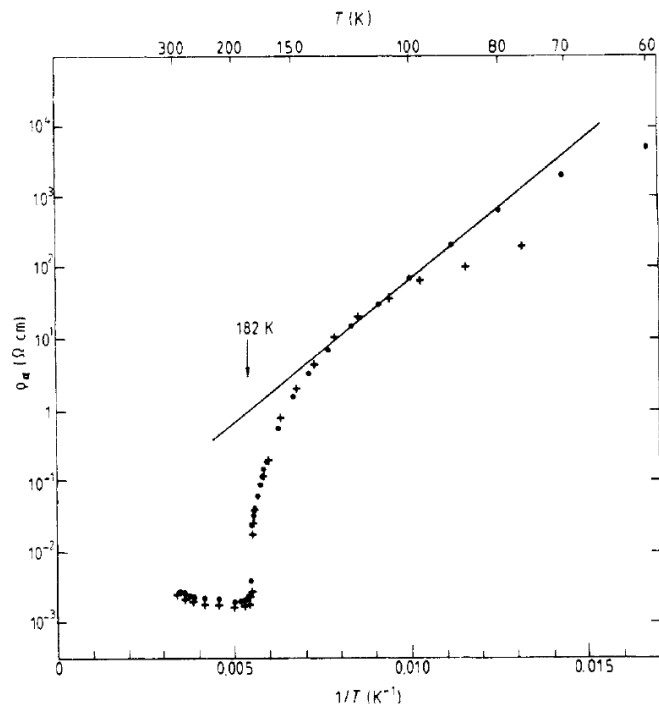


FIG. 1. The resistivity as a function of temperature for  $\text{NbSe}_2$ .

## $\text{NbSe}_2$

# Density-wave-Like

Anion ordering: big “external” periodic potential with periodicity close to  $2K_F$





# Almost all high-T<sub>c</sub> materials have unusual ρ(T) Electrons pair as they scatter!

PHYSICAL REVIEW B

VOLUME 15, NUMBER 5

1 MARCH 1977

## Apparent $T^2$ dependence of the normal-state resistivities and lattice heat capacities of high- $T_c$ superconductors\*

G. W. Webb, Z. Fisk, and J. J. Engelhardt

Institute for Pure and Applied Physical Sciences, University of California, San Diego, La Jolla, California 92093

S. D. Bader

Argonne National Laboratory, Argonne, Illinois 60439

(Received 8 March 1976; revised manuscript received 17 September 1976)

We report new measurements of the normal-state electrical resistances of several high- $T_c$  ( $\sim 20$  K) A-15 structure superconductors. It is found that the resistances are linear functions of  $T^2$  from  $T_c$  to 40 K. Analysis of available lattice heat-capacity data on the same materials shows that it also varies as  $T^2$  over the same temperature interval. These observations suggest that the  $T^2$  resistivity is due to electron-phonon scattering. This interpretation is supported by the results of a model calculation for the temperature dependence of the resistivity and the lattice-heat capacity of Nb<sub>3</sub>Sn.

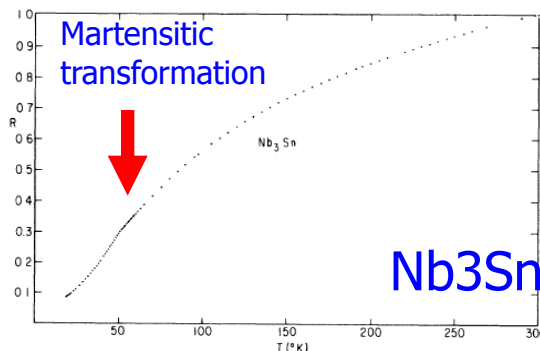


FIG. 1. Resistance of Nb<sub>3</sub>Sn from  $T_c$  (18.2 K) to 300 K in units where  $R$  (300 K) = 1.0. The kink at 51 K is indicative of a martensitic transformation. Using the data of Woodward and Cody we estimate  $\rho$  (300 K) = 75  $\mu\Omega \text{ cm}$ .

Strong electron-phonon interaction

Unusual  $\rho(T)$  dependence: saturation at high  $T$ , Low  $T$ - extended range of  $T^2$  behavior

Correlating with  $T^2$  (rather than  $T^3$ )  
lattice specific heat

## Systematic Evolution of Temperature-Dependent Resistivity in $\text{La}_{2-x}\text{Sr}_x\text{CuO}_4$

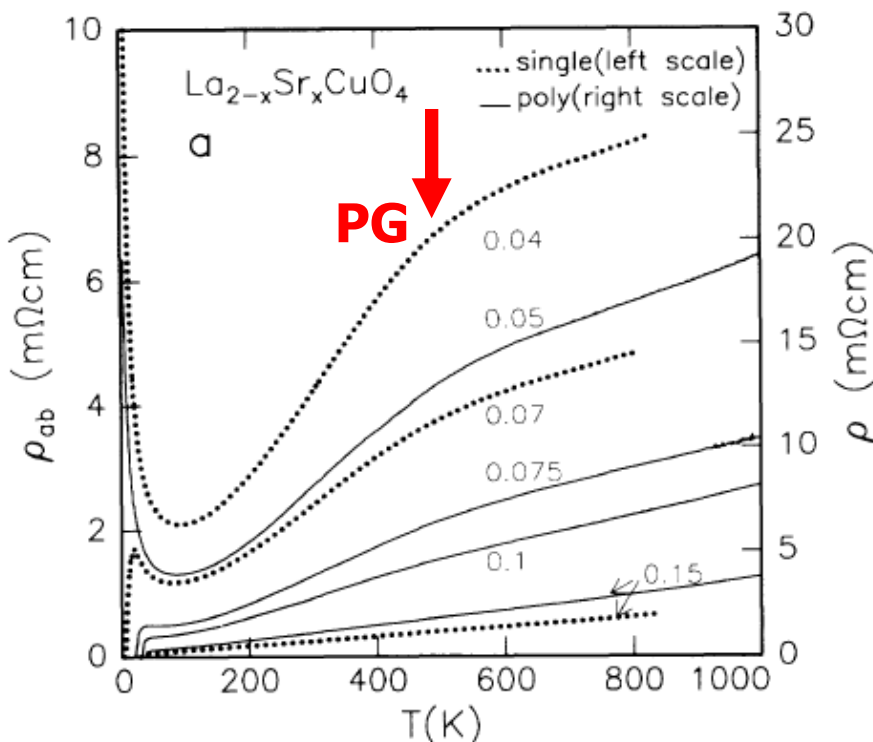
H. Takagi, B. Batlogg, H. L. Kao, J. Kwo, R. J. Cava, J. J. Krajewski, and W. F. Peck, Jr.

*AT&T Bell Laboratories, Murray Hill, New Jersey 07974*

(Received 8 May 1992)

$\text{La}_{2-x}\text{Sr}_x\text{CuO}_4$

$X=0 - 0.15$



$\rho \sim T$  at optimal doping  
 $\rho \sim T^n$  at higher dopings

$X=0.1 - 0.35$

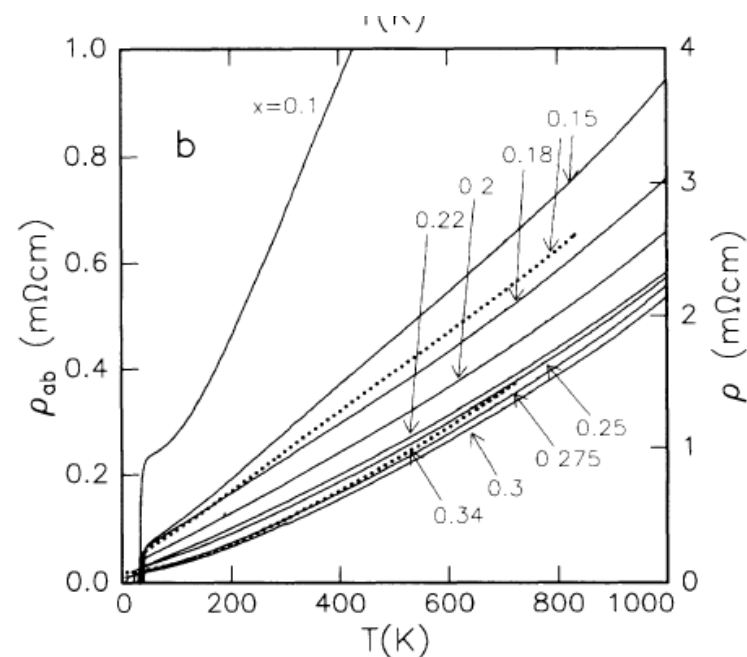


FIG. 1. The temperature dependence of the resistivity for  $\text{La}_{2-x}\text{Sr}_x\text{CuO}_4$ . (a)  $0 < x \leq 0.15$ , (b)  $0.1 \leq x < 0.35$ . Dotted lines, the in-plane resistivity ( $\rho_{ab}$ ) of single-crystal films with (001) orientation; solid lines, the resistivity ( $\rho$ ) of polycrystalline materials. Note,  $\rho_M = (h/e^2)d = 1.7 \text{ m}\Omega\text{ cm}$ .



$\text{La}_{2-x}\text{Sr}_x\text{CuO}_4$

## C-axis transport

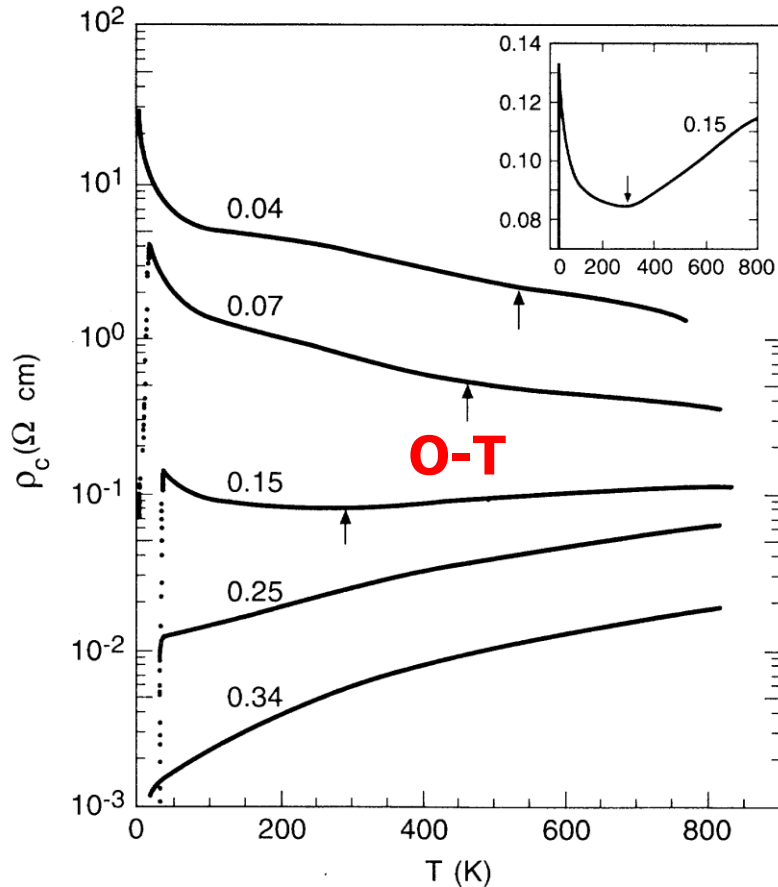


FIG. 3. Semilog plots of  $\rho_c$  vs  $T$  for  $x = 0.04, 0.07, 0.15, 0.25$ , and  $0.34$ . The inset shows the linear plot of  $\rho_c$  for  $x = 0.15$ . The arrows denote the temperature of the orthorhombic-to-tetragonal transformation where a discontinuous change of  $d\rho_c/dT$  appears.

## Highest T<sub>c</sub> heavy fermion CeCoIn<sub>5</sub>

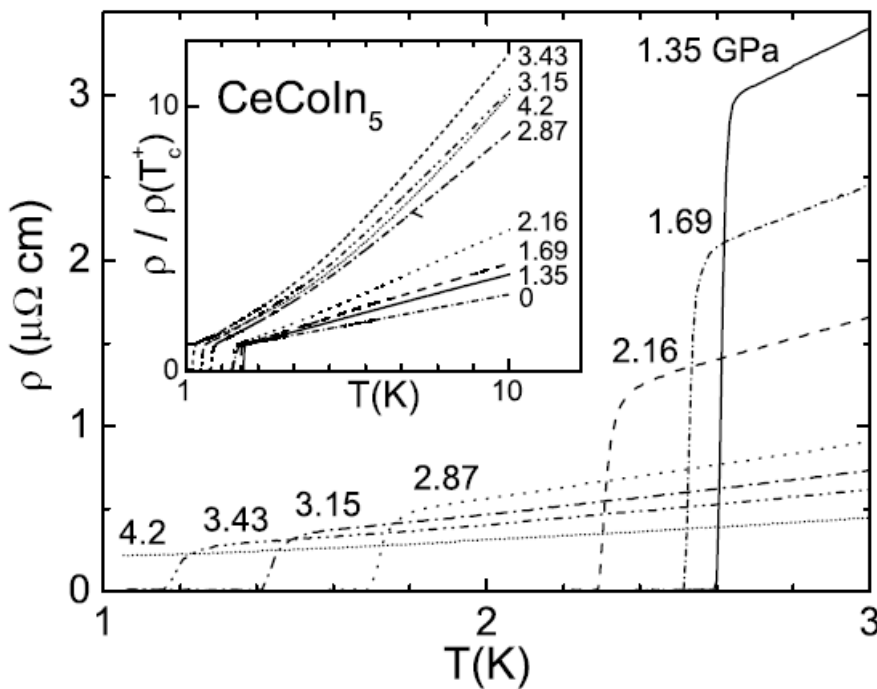


FIG. 1. Effect of pressure on the low-temperature resistivity and superconducting  $T_c$  of CeCoIn<sub>5</sub>. The inset shows the resistivity  $\rho$  normalized by  $\rho(T_c^+)$  up to 10 K.

## Highest T<sub>c</sub> organic superconductors

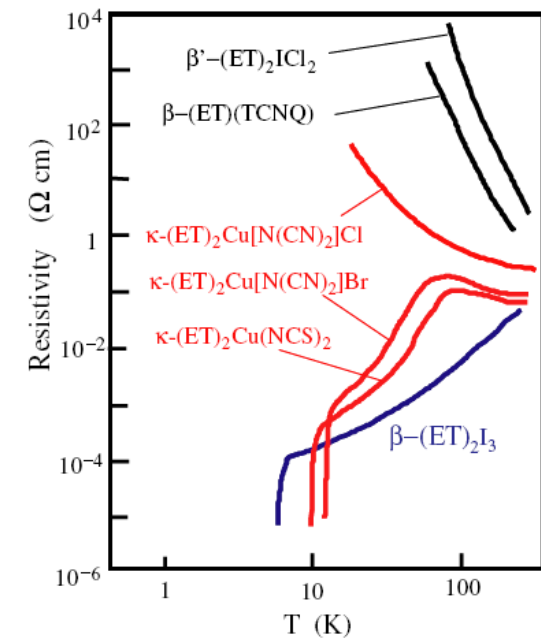


Fig. 2. (Color online) Resistivity behaviors of  $\kappa-(ET)_2X$  and related dimeric compounds.